Received: 19 April 2024 | Revised: 19 June 2024 | Accepted: 21 July 2024

DOI: 10.1002/mma.10381

RESEARCH ARTICLE

WILEY

On the analyzing of bifurcation properties of the one-dimensional Mackey–Glass model by using a generalized approach

Shuai Zhang[1] | **Yaya Wang**[2] | **Hongyin Geng**[1] | **Wei Gao**[3] | **Esin Ilhan**[4] | **Haci Mehmet Baskonus**[5]

[1]Internship and Training Management Division, Binzhou Polytechnic, Binzhou, China

[2]Department of Information Engineering, Binzhou Polytechnic, Binzhou, China

[3]School of Information Science and Technology, Yunnan Normal University, Kunming, China

[4]Faculty of Engineering and Architecture, Kirsehir Ahi Evran University, Kirsehir, Turkey

[5]Department of Mathematics and Science Education, Faculty of Education, Harran University, Sanliurfa, Turkey

Correspondence
Haci Mehmet Baskonus, Department of Mathematics and Science Education, Faculty of Education, Harran University, Sanliurfa, Turkey.
Email: hmbaskonus@gmail.com

Communicated by: P. Agarwal

Funding information
There are no funders to report for this submission.

The goal of this work is to look at how a nonlinear model describes hematopoiesis and its complexities utilizing commonly used techniques with historical and material links. Based on time delay, the Mackey–Glass model is explored in two instances. To offer a range, the relevance of the parameter impacting stability (bifurcation) is recorded. The power spectrum of the considered model is collected in order to analyze the periodic behavior of a solution in a differential equation. The complex nature of the system is relayed on a parameter which is illustrated in the bifurcation plot. Due to the fact that the considered model is associated with blood-related diseases, the effect coefficients are effectively captured. The corresponding parameters-based consequences of the generalized model in different order are deduced. The parametric charts for both examples reveal intriguing results. The current work enables investigations into complex real-world problems as well as forecasts of essential techniques.

KEYWORDS

bifurcation, Caputo fractional derivative, hematopoiesis, numerical method

MSC CLASSIFICATION

35A20, 35A24, 37M99, 34C11

1 | INTRODUCTION

The most effective tools for analyzing complicated issues in physics, chemistry, and biology are numerical approaches and mathematical modeling [1, 2]. Recently, it has become more common to find research articles in the literature that explain the fundamentals and effects of differential equations, particularly ordinary differential equations, which appear straightforward but are dependent on a single independent variable and can only provide a chaotic nature. Since Lorentz first noticed this chaotic behavior in electron interactions, scientists have attempted to comprehend this interesting aspect of dynamical systems. Researchers are interested in these systems because they display the butterfly effect and asymptotic stability. However, this interest has also led to the development of several tools that facilitate effective analysis of these models [3–6].

Chaotic behavior has been seen in several disciplines of science, including optics, climate, earthquakes, epidemics, fluid mechanics, and quantum mechanics. The Lorenz attractor [7] is a collection of chaotic solutions to a set of differential equations representing atmospheric convection. Chaotic behavior may be seen in a wide range of physical systems. It may be identified by how sensitive the system's behavior is to the initial conditions. The significance of chaotic behavior in physics stems from its ability to describe complicated phenomena that are inexplicable using traditional methods. Chaotic systems can exhibit a variety of behaviors, including periodic orbits, quasiperiodic orbits, and odd attractors [8, 9].

Many studies collectively highlight the extensive use of fractional calculus (FC) in modeling and analyzing complex systems across various domains. Mohammadi et al. [10] develop a Caputo–Fabrizio fractional model to control hearing loss due to the Mumps virus, while Chakraborty and Veeresha [11] investigate chaos dynamics and control in a transformed fractional Samardzija–Greller framework. Baleanu et al. [12] employ the Laplace Adomian decomposition method to model epidemic childhood diseases using Caputo–Fabrizio derivatives. Khan et al. [13] focus on the fractal-fractional tuberculosis model in China, examining its existence and stability theories through numerical simulations. Additional studies by Baleanu, Etemad, and colleagues [14] model boundary value problems on the glucose graph, and by Baleanu et al. [15] apply Caputo-Fabrizio fractional derivatives to human liver modeling. Tuan et al. [16] use Caputo fractional derivatives to model COVID-19 transmission, while Chakraborty and Veeresha [17] study global warming and chaos control in atmospheric propagation models. Hussain et al. [18] investigate stochastic modeling of COVID-19 with environmental noise, while Ahmad et al. [19] examine the stability of neutral stochastic fractional differential systems. Raghavendra and Veeresha [20] analyze digital payment markets in India using a predator-prey model. Khan et al. [21] present a fractal-fractional waterborne disease model, exploring theoretical and numerical solutions. Aydogan et al. [22] use Caputo-Fabrizio fractional derivatives to model Rabies, and Gao et al. [23] apply iterative methods to fractional thermoelasticity systems with Mittag-Leffler kernels. Finally, Dehingia et al. [24] investigate the dynamical behavior of within-host SARS-CoV-2 using fractional order models. Many researchers captured some interesting behaviors underscoring the broad applicability of FC in addressing diverse scientific challenges [25, 26].

The one-dimensional Mackey–Glass model is based on a system of delay differential equations (DDEs) that describe the dynamics of hematopoietic stem cells and their progeny [27]. The model assumes that stem cells divide asymmetrically to produce two types of progeny: self-renewing stem cells and differentiating progenitor cells. One of the key features of the one-dimensional Mackey–Glass model is the presence of feedback mechanisms that regulate the production of blood cells. In this model, the production of blood cells is regulated by a feedback mechanism that involves the concentration of mature blood cells in the bloodstream. When the concentration of blood cells is low, the feedback mechanism stimulates the production of new blood cells. Conversely, when the concentration of blood cells is high, the feedback mechanism inhibits the production of new blood cells. The model has been used to study the effects of various perturbations on hematopoietic dynamics, such as chemotherapy-induced damage to the bone marrow. Studies using the model have shown that chemotherapy can disrupt the delicate balance between stem cell self-renewal and differentiation, leading to a depletion of stem cells and a reduction in blood cell production. Overall, the one-dimensional Mackey–Glass model provides a useful tool for studying the dynamics of hematopoiesis and understanding the mechanisms regulating blood cell production in health and disease. Further research using this model could lead to new insights into the treatment of blood disorders and the development of new therapies for blood-related diseases [28–30].

In concerned with the essence of modeling the phenomena associated with daily life help appreciate the understanding blood cell population $\mathcal{B}(t)$, the following ordinary differential equation without time delay is presented as follows with a death rate of blood cells μ

$$\frac{d\mathcal{B}}{dt} - \frac{\alpha\, \mathcal{B}(t)}{1 + \mathcal{B}(t)^{\kappa}} + \mu\mathcal{B}(t) = 0. \tag{1}$$

DDEs are used to simulate time delay in differential equations. DDEs are used to represent systems in which the current state is dependent on previous states. The time delay may have a substantial influence on a system's behavior, causing oscillations, instability, and other complicated dynamics [31, 32]. In all the studies, the authors consider the delay effect or time lag (τ) in Equation (1) with the constant κ, as follows [33]:

$$\frac{d\mathcal{B}}{dt} = \frac{\alpha\, \mathcal{B}(t-\tau)}{1 + \mathcal{B}(t-\tau)^{\kappa}} - \mu\mathcal{B}(t). \tag{2}$$

Since the above equation helps us to understand more interesting behavior the real-world problems, the authors consider two constant time delays (namely, τ_1 and τ_2) [33]

$$\frac{d\mathcal{B}}{dt} = \frac{\alpha\,(\mathcal{B}(t-\tau_1) + \mathcal{B}(t-\tau_2))}{1 + (\mathcal{B}(t-\tau_1) + \alpha\mathcal{B}(t-\tau_2))^{\kappa}} - \mu\mathcal{B}(t). \tag{3}$$

In order to create a perfect and effective model of the complex nature, humanity selected the greatest tools for studying and documenting the resulting impacts. Despite the fact that employing both integral and differential operators, calculus theory has been shown to be the most precise and effective way to study and analyze these occurrences. The connected system's shortcomings and the necessity to generalize it to encompass additional significant physical aspects related to time, hereditary, historical, and material properties were frequently brought up by scholars during the 20th century. Due to their curious thinking, a lot of academics have recently been interested in FC, which goes back to 1695 [34, 35].

Scientifically speaking, FC offers a more plausible explanation of nonlinear, nonlocal, and memory-dependent behavior in physical systems, enabling the extension of conventional real-world models to fractional order models. Traditional models based on integer-order differential equations make the mistake of thinking the process under study instantaneous and memory-free, which is generally not the case in reality. Systems having memory, nonlocality, and nonlinearity can be described mathematically using FC. In many situations where typical integer order models fall short of adequately describing the behavior of the system, such as in signal processing, control engineering, and biomedical systems, fractional order models have been successfully used.

FC is a theoretical area with minimal room for innovation and a reputation for challenging theoretical submissions, according to a number of scholars. However, Michele Caputo's method from 1967 mentions has had a considerable impact on the concept of FC [36], despite the fact that the majority of them believe that present restrictions are mostly to blame for the tool's shortcomings [37–39]. The Caputo operator is the sole tool that can be used to generalize the majority of the newly suggested notations. Moreover, several scholars investigate other theories in regard to this operator cited in [40, 41]. A number of young academics' careers were influenced by the appraisal of both the new and the old fractional operators [42–46].

Here, we employed the Adams–Bashforth–Moulton (ABM) technique [47, 48]. Many scientists employ this technique to examine complex phenomena, and the recommended procedure is especially useful in researching ODEs [49–51]. From Equation (2), we have

$$D_t^{\rho}\mathcal{B}(t) = \frac{\alpha\,\mathcal{B}(t-\tau)}{1+\mathcal{B}(t-\tau)^{\kappa}} - \mu\mathcal{B}(t). \tag{4}$$

The corresponding fractional order equation for Equation (3) is

$$D_t^{\rho}\mathcal{B}(t) = \frac{\alpha\left(\mathcal{B}(t-\tau_1)+\mathcal{B}(t-\tau_2)\right)}{1+\left(\mathcal{B}(t-\tau_1)+\alpha\mathcal{B}(t-\tau_2)\right)^{\kappa}} - \mu\mathcal{B}(t). \tag{5}$$

Here, ρ is the fractional order. A bifurcation diagram depicts the qualitative changes in the behavior of a dynamical system as one or more parameters are altered. It is used to examine the stability of differential equation solutions and to identify the critical parameter values that cause qualitative changes. It has been testified by researchers reading the parameter in the considered model

2 | PRELIMINARIES

Theorems and findings used to examine the system's stability and boundedness are presented in this section.

Definition 2.1 ([52])**.** Let $f(t)$ be 'n' times continuously differentiable function. Then the ρ order Caputo fractional derivative is defined as

$${}_{t_0}^{C}D_t^{\rho}f(t) = \frac{1}{\Gamma(n-\rho)}\int_{t_0}^{t}\frac{f^{(k)}(\varsigma)}{(t-\varsigma)^{\rho+1-n}}d\varsigma, n-1<\rho<n, \tag{6}$$

where the Gamma function is denoted by $\Gamma(\cdot)$.

Lemma 2.2 ([53])**.** *For the system*

$${}_{t_0}^{C}D_t^{\rho}y(t) = g(t,y), t > t_0, \tag{7}$$

with the initial condition $y(t_0)$, where $0<\rho\le 1$ and $g:[t_0,\infty]\times\Psi\to\mathbb{R}^n, \Psi\in\mathbb{R}^n$. There exists only one solution of Equation (7) on $[t_0,\infty)\times\Psi$ if the local Lipchitz condition with respect to y is followed by $g(t,x)$.

Lemma 2.3. ([54]). *Let $g(t)$ be a continuous function on $[t_0, +\infty)$ and satisfying*

$$ {}_{t_0}^{C}D_t^{\rho} g(t) \leq -\psi g(t) + \nu, g(t_0) = g_0(t). \tag{8} $$

Here, $0 < \rho \leq 1$, $(\psi, \nu) \in \mathbb{R}^2$, $\psi \neq 0$ and $t_0 \geq 0$ is the initial time. Then

$$ g(t) \leq \left(g(t_0) - \frac{\nu}{\psi} \right) E_{\rho}[-\psi(t - t_0)^{\rho}] + \frac{\nu}{\psi}. \tag{9} $$

Lemma 2.4. ([55]). *The equilibrium y_0 is globally stable if a function $G(y)$ is globally positively definite, radially unbounded, and its time derivative is globally negative, $G'(y) < 0$ for all $y \neq y_0$.*

3 | BOUNDEDNESS

Boundedness is significant since it implies that the system will not continue to develop or degrade endlessly. A dynamical system is considered to be limited if its state variables stay inside a given range or region of the phase space across time. The boundedness of the solutions of Equation (4) is established as follows:

Theorem 3.1. *The solution for Equation (4) is uniformly bounded.*

Proof. Consider

$$ \begin{aligned} {}_{t_0}^{C}D_t^{\rho} \mathcal{B}(t) + \hbar(t) &= {}_{t_0}^{C}D_t^{\rho} \mathcal{B}(t) + \hbar(t)\mathcal{B}(t) \\ &= \frac{\alpha\, \mathcal{B}(t-\tau)}{1 + \mathcal{B}(t-\tau)^{\kappa}} - \mu \mathcal{B}(t) + \hbar(t)\mathcal{B}(t) \\ &\leq \frac{\alpha\, \mathcal{B}(t-\tau)}{1 + \mathcal{B}(t-\tau)^{\kappa}} + \hbar(t)\mathcal{B}(t). \end{aligned} \tag{10} $$

The solution exists and is unique in

$$ \Lambda = \{ \mathcal{B}(t-\tau) : max\{(\mathcal{B}(t-\tau)|\} \leq \mathcal{N} \}. \tag{11} $$

Then

$$ {}_{t_0}^{C}D_t^{\rho} \mathcal{B}(t) + \hbar(t) \leq + \left(\frac{\alpha}{1 + \mathcal{N}^{\kappa}} + \hbar(t) \right) \mathcal{N}. $$

By Lemma 2.3, we get

$$ {}_{t_0}^{C}D_t^{\rho} \mathcal{B}(t) \leq \left(\mathcal{B}(t_0) - \frac{1}{\hbar(t)} \left(\frac{\alpha}{1 + \mathcal{N}^{\kappa}} + \hbar(t) \right) \mathcal{N} \right) E_{\rho}(-\theta(t - t_0)^{\rho}). $$

Then

$$ {}_{t_0}^{C}D_t^{\rho} \mathcal{B}(t) \to \left(\frac{\alpha}{1 + \mathcal{N}^{\kappa}} + \hbar(t) \right) \mathcal{N}, t \to \infty. $$

It confirms that the solution of Equation (4) remained bounded in

$$ \Xi = \left\{ \mathcal{B} \in \Lambda | N(t) \leq \left(\frac{\alpha}{1 + \mathcal{N}^{\kappa}} + \hbar(t) \right) \mathcal{N} + \epsilon, \epsilon > 0 \right\}. $$

□

4 | EXISTENCE AND UNIQUENESS OF THE SOLUTIONS

The existence and distinctness of the solutions to the proposed model are shown in this section using the Banach fixed-point theorem. Then by (4), we have

$$D_t^{\rho}[\mathcal{B}(t)] = \mathcal{G}(t, \mathcal{B}). \tag{12}$$

With a Volterra-type integral equation, we have

$$\mathcal{B}(t) - \mathcal{B}(t_0) = \frac{1}{\Gamma(\rho)} \int_{t_0}^{t} \mathcal{G}_1(\vartheta, \mathcal{B})(t-\vartheta)^{\rho-1} d\vartheta. \tag{13}$$

Theorem 4.1. *The kernel $\mathcal{G}_1$ holds the Lipschitz condition and contraction if $0 \leq \left(\frac{\alpha(\lambda_1-\lambda_2+\lambda_1\lambda_2^{\kappa}-\lambda_1^{\kappa}\lambda_2)}{(1+\lambda_1^{\kappa})(1+\lambda_2^{\kappa})} - \mu\right) < 1$ holds.*

Proof. We shall consider the two functions $\mathcal{B}$ and $\mathcal{B}_1$ such as:

$$\begin{aligned}
\|\mathcal{G}(t, \mathcal{B}) - \mathcal{G}(t, \mathcal{B}_1)\| &= \left\| \left(\frac{\alpha\, \mathcal{B}(t)}{1 + \mathcal{B}(t)^{\kappa}} - \mu \mathcal{B}(t) \right) - \left(\frac{\alpha\, \mathcal{B}(t_1)}{1 + \mathcal{B}(t_1)^{\kappa}} - \mu \mathcal{B}(t_1) \right) \right\| \\
&\leq \| \left(\frac{\alpha(\mathcal{B}(t) - \mathcal{B}(t_1) + \mathcal{B}(t)\mathcal{B}^{\kappa}(t_1) - \mathcal{B}^{\kappa}(t)\mathcal{B}(t_1))}{(1 + \mathcal{B}^{\kappa}(t))(1 + \mathcal{B}^{\kappa}(t_1))} - \mu \right) \| \, \|\mathcal{B}(t) - \mathcal{B}(t_1)\| \\
&\leq \left(\frac{\alpha(\lambda_1 - \lambda_2 + \lambda_1\lambda_2^{\kappa} - \lambda_1^{\kappa}\lambda_2)}{(1 + \lambda_1^{\kappa})(1 + \lambda_2^{\kappa})} - \mu \right) \|\mathcal{B}(t) - \mathcal{B}(t_1)\| \\
&\leq \zeta ||\mathcal{B}(t) - \mathcal{B}(t_1)||,
\end{aligned} \tag{14}$$

where $||\mathcal{B}(t)|| \leq \lambda_1$ and $||\mathcal{B}(_1 t)|| \leq \lambda_2$. Taking $\zeta = \frac{\alpha(\lambda_1-\lambda_2+\lambda_1\lambda_2^{\kappa}-\lambda_1^{\kappa}\lambda_2)}{(1+\lambda_1^{\kappa})(1+\lambda_2^{\kappa})} - \mu$, we have

$$||\mathcal{G}(t, \mathcal{B}) - \mathcal{G}(t, \mathcal{B}_1)|| \leq \zeta ||\mathcal{B} - \mathcal{B}(t_1)||. \tag{15}$$

Therefore, $\mathcal{G}$ satisfies the Lipschitz condition, and if $0 \leq \left(\frac{\alpha(\lambda_1-\lambda_2+\lambda_1\lambda_2^{\kappa}-\lambda_1^{\kappa}\lambda_2)}{(1+\lambda_1^{\kappa})(1+\lambda_2^{\kappa})} - \mu\right) < 1$, then it follows a contraction. Now, by Equation (13), the recursive form is

$$\mathcal{B}_n(t) = \mathcal{B}_0(t) + \frac{1}{\Gamma(\rho)} \int_{t_0}^{t} \mathcal{G}_1(\vartheta, \mathcal{B}_{n-1})(t-\vartheta)^{\rho-1} d\vartheta, \tag{16}$$

with

$$\mathcal{B}_0(t) = \mathcal{B}(t_0).$$

Then by the successive terms difference, we have

$$\aleph_n(t) = \mathcal{B}_n(t) - \mathcal{B}_{n-1}(t) = \frac{1}{\Gamma(\rho)} \int_{t_0}^{t} (\mathcal{G}_1(\vartheta, \mathcal{B}_{n-1}) - \mathcal{G}_1(\vartheta, \mathcal{B}_{n-2}))(t-\vartheta)^{\rho-1} d\vartheta.$$

Notice that

$$\mathcal{B}_n(t) = \sum_{i=1}^{n} \aleph_i(t).$$

Applying norm on system (17) and then using Equation (15), we have

$$||\aleph_n(t)|| \leq \frac{1}{\Gamma(\rho)} \zeta \int_{t_0}^{t} ||\aleph_{n-1}(\vartheta)|| d\vartheta. \tag{17}$$

By using the above theorem, we prove the following results. □

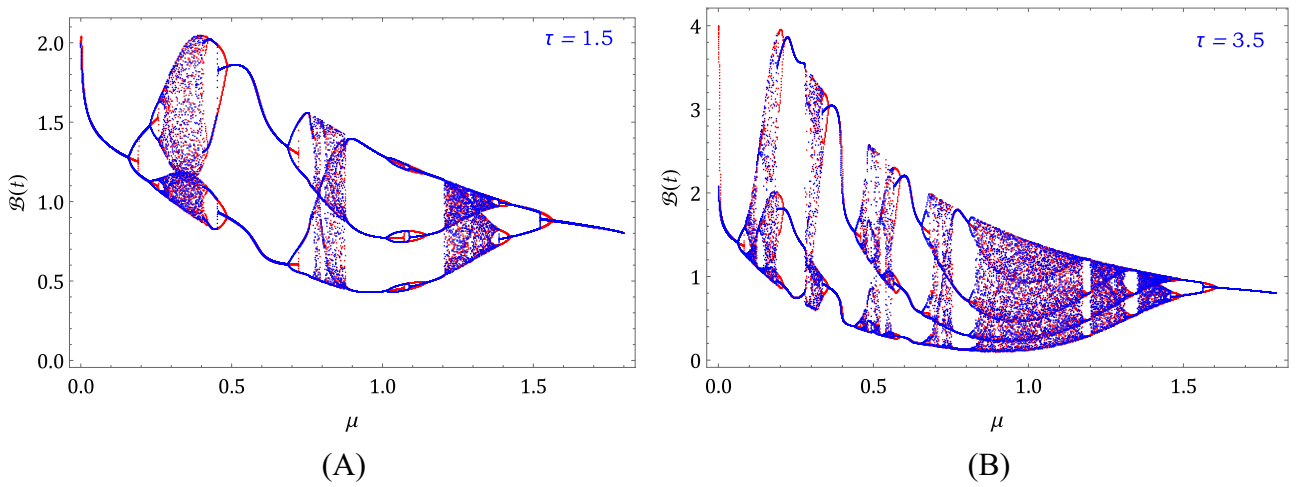

FIGURE 1 Bifurcation for Equation (4) at $\alpha = 2, \kappa = 10$ and $\rho = 1$ with (A) $\tau = 1.5$ and (B) $\tau = 3.5$. [Colour figure can be viewed at wileyonlinelibrary.com]

Theorem 4.2. *The solution of Equation (4) will exist and is unique if we obtain some t_0 such that*

$$\frac{1}{\Gamma(\rho)}\zeta t_0 < 1.$$

Proof. Let $\mathcal{B}(t)$ is the bounded function which satisfy the Lipschitz condition. Now, by Equation (17), we have

$$||\aleph_i(t)|| \leq ||\mathcal{B}_n(t_0)||\left[\frac{1}{\Gamma(\rho)}\zeta\right]^n.$$

Hence, both the existence and continuity are shown for the obtained solutions. To prove that relation (4) is the solution for (4), we consider

$$\mathcal{B}(t) - \mathcal{B}(t_0) = \mathcal{B}_n(t) - \mathfrak{W}_{1n}(t).$$

Now, we set

$$\begin{aligned} ||\mathfrak{W}_n(t)|| &= ||\frac{1}{\Gamma(\rho)}\int_{t_0}^{t}(t-\vartheta)^{\rho-1}(\mathcal{G}_1(\vartheta,\mathcal{B}) - \mathcal{G}_1(\vartheta,\mathcal{B}_{n-1}))d\vartheta|| \\ &\leq \frac{1}{\Gamma(\rho)}\int_{t_0}^{t}(t-\vartheta)^{\rho-1}||(\mathcal{G}_1(\vartheta,\mathcal{B}) - \mathcal{G}_1(\vartheta,\mathcal{B}_{n-1}))||d\vartheta \\ &\leq \frac{1}{\Gamma(\rho)}\zeta||\mathcal{B} - \mathcal{B}_{n-1}||t. \end{aligned} \tag{18}$$

At t_0, we get

$$||\mathfrak{W}_n(t)|| \leq \left(\frac{t_0}{\Gamma(\rho)}\right)^{n+1}\zeta^{n+1}M. \tag{19}$$

From Equation (19), we can see that as n tends to ∞, $||\mathfrak{W}_n(t)||$ approaches to 0 provided $\frac{t_0}{\Gamma(\rho)} < 1$.
We prove uniqueness on contrary, if there exists other set of solutions $\mathcal{B}^*(t)$. Then

$$\mathcal{B}(t) - \mathcal{B}^*(t) = \frac{1}{\Gamma(\rho)}\int_{t_0}^{t}(\mathcal{G}_1(\vartheta,\mathcal{B}) - \mathcal{G}_1(\vartheta,\mathcal{B}^*))d\vartheta.$$

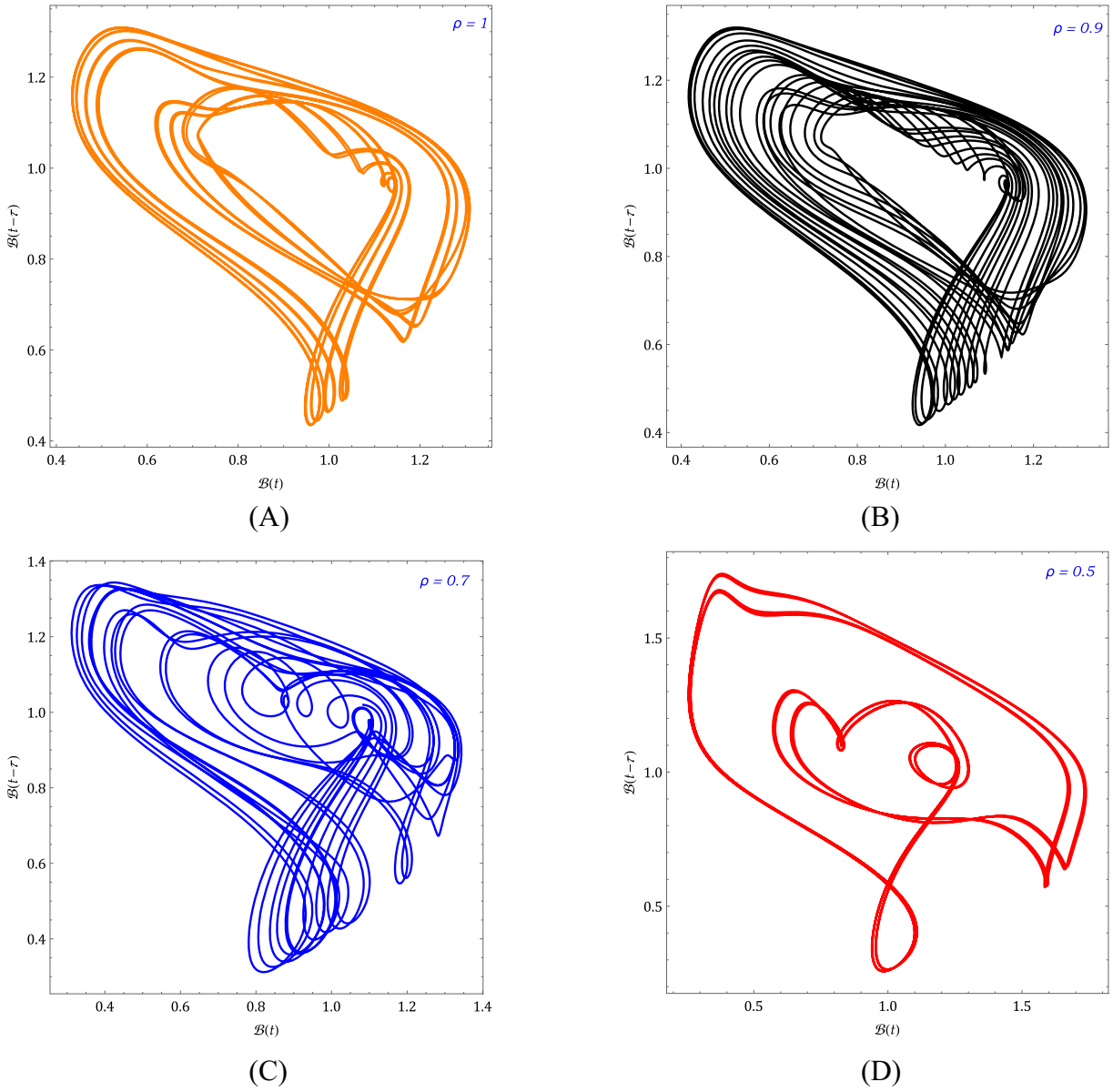

FIGURE 2 Parametric nature for Equation (4) at ρ is (A) 1, (B) 0.9, (C) 0.7, and (D) 0.5 combined with $\kappa = 10, \tau = 1.5, \mu = 1$, and $\alpha = 2$. [Colour figure can be viewed at wileyonlinelibrary.com]

By employing the norm, the above equation becomes

$$\begin{aligned} ||\mathcal{B}(t) - \mathcal{B}^*(t)|| &= ||\frac{1}{\Gamma(\rho)} \int_{t_0}^{t} (\mathcal{G}_1(\vartheta, \mathcal{B}) - \mathcal{G}_1(\vartheta, \mathcal{B}^*)) d\vartheta|| \\ &\leq \frac{1}{\Gamma(\rho)} \zeta t ||\mathcal{B} - \mathcal{B}^*(t)||. \end{aligned} \tag{20}$$

For some t_0, one can get

$$||\mathcal{B}(t) - \mathcal{B}^*(t)|| \left(1 - \frac{1}{\Gamma(\rho)} \zeta t_0\right) \leq 0.$$

Since

$$\left(1 - \frac{1}{\Gamma(\rho)} \zeta t\right) \geq 0, \tag{21}$$

from the above inequality, it is clear that $\mathcal{B}(t) - \mathcal{B}^*(t) = 0$. Hence, Equation (21) proves the required result. □

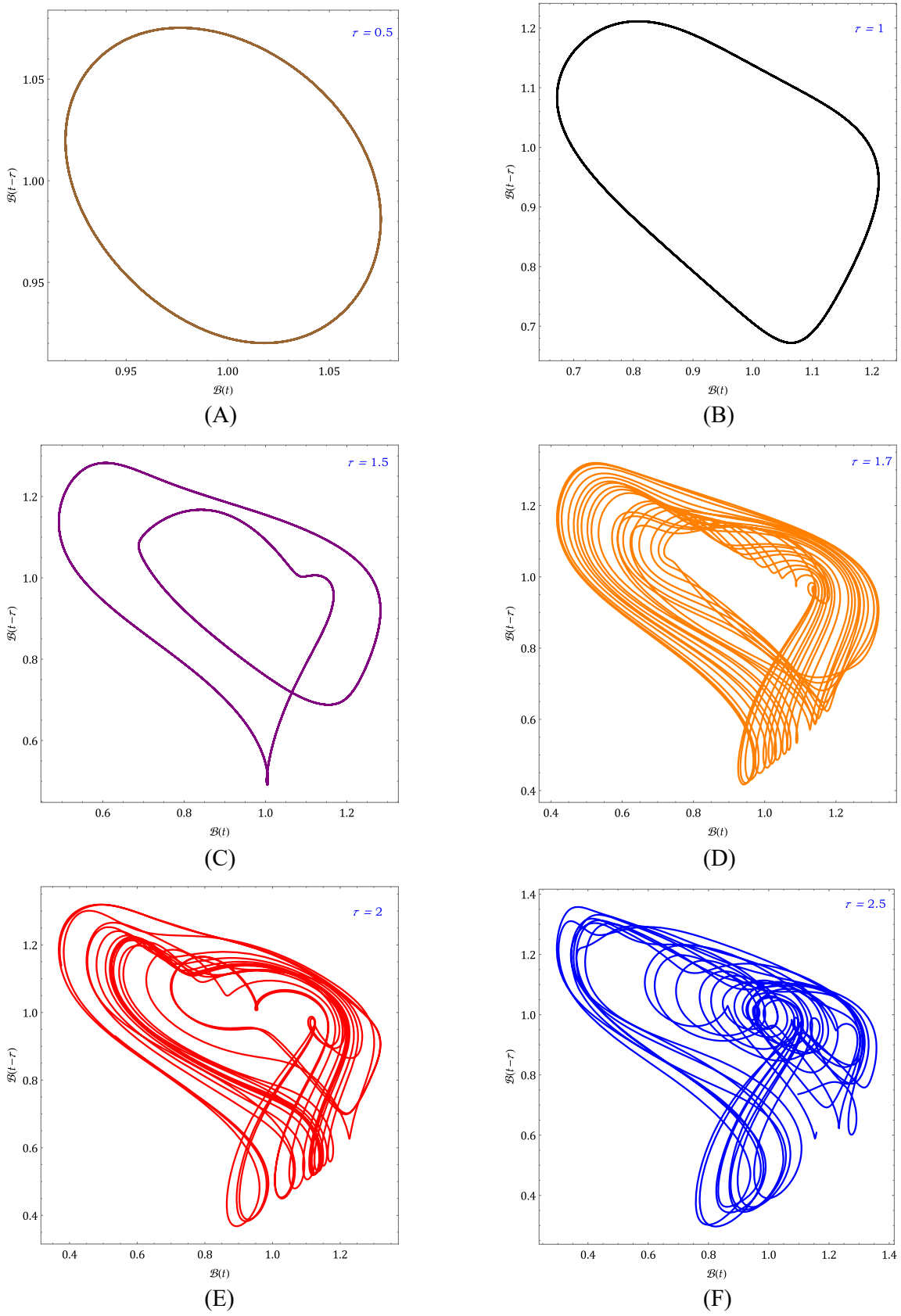

FIGURE 3 Parametric nature for Equation (4) at τ is (A) 0.5, (B) 1, (C) 1.5, (D) 1.7, (E) 2, and (F) 2.5 combined with $\kappa = 10$, $\mu = 1$, $\rho = 1$, and $\alpha = 2$. [Colour figure can be viewed at wileyonlinelibrary.com]

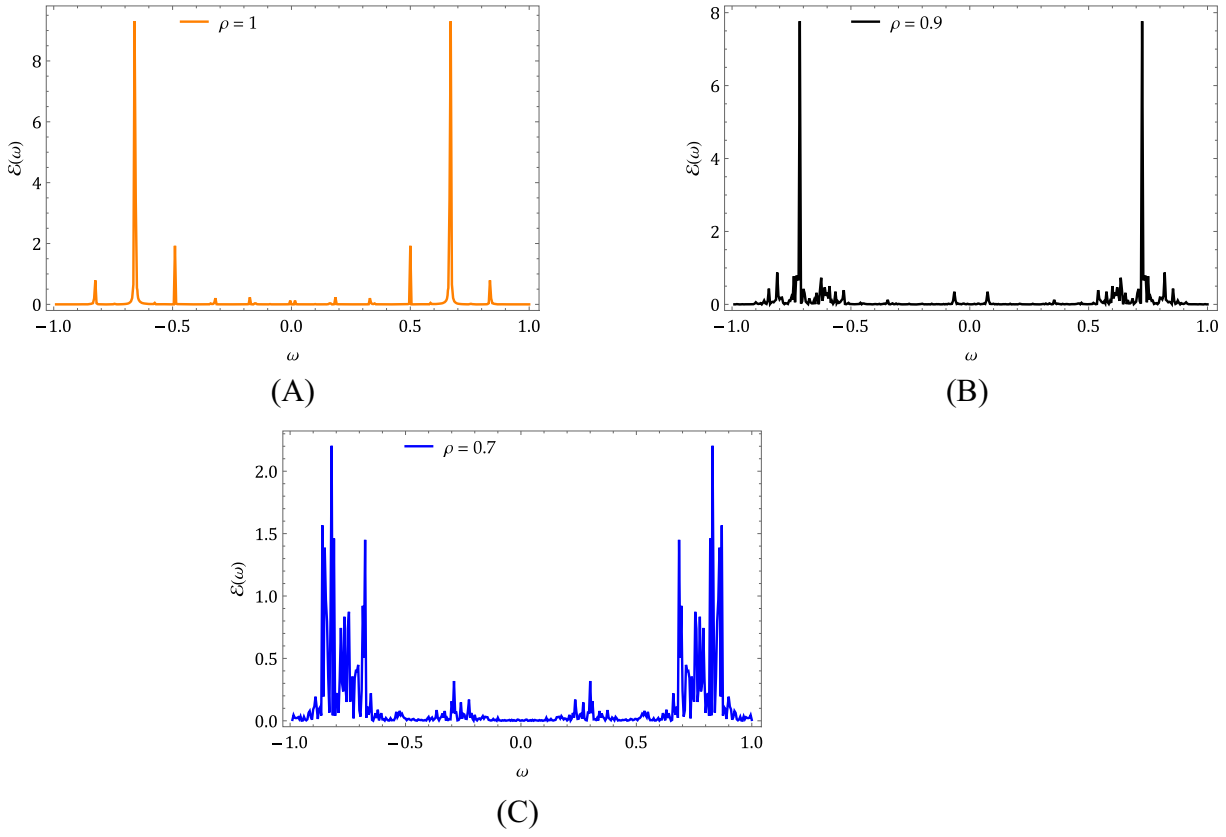

FIGURE 4 The power spectrum behavior of the Equation (4) at $\alpha = 2, \mu = 0.8, \tau = 2$, and $\kappa = 10$ for ρ is (A) 1, (B) 0.9, and (C) 0.7. [Colour figure can be viewed at wileyonlinelibrary.com]

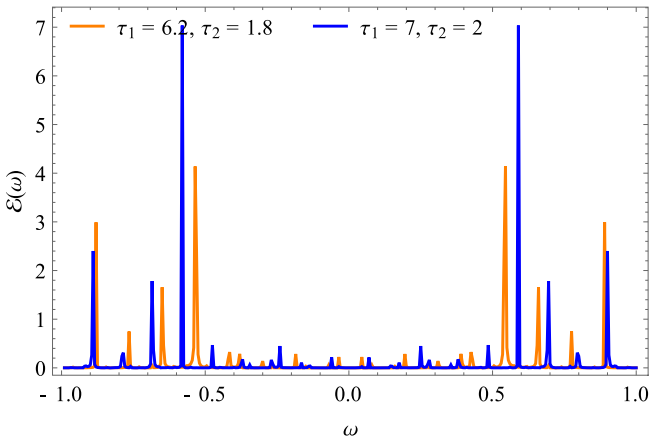

FIGURE 5 The power spectrum behavior of Equation (5) at $\alpha = 2, \mu = 0.8$. [Colour figure can be viewed at wileyonlinelibrary.com]

5 | NUMERICAL METHOD

In this segment, the ABM method is used to analyze the projected model. Now, consider

$$\begin{aligned} {}^{C}D_t^{\rho} y(t) &= \phi(t, y(t)), \ 0 \le t \le T, \\ y^{(m)}(0) &= y_0^{(m)}, \ m = 0, 1, 2, 3, \ \ldots \ , \nu, \ \nu = \lceil \rho \rceil. \end{aligned} \tag{22}$$

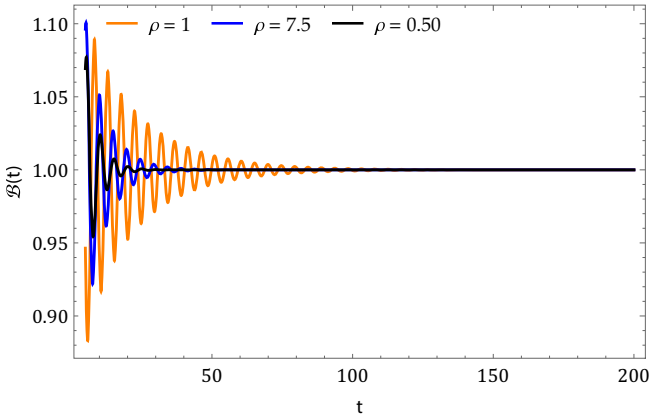

FIGURE 6 The power spectrum behavior of the Equation (4) at $\alpha = 2$, $\mu = 0.8$, $\tau = 1.656$, and $\kappa = 10$ for different ρ. [Colour figure can be viewed at wileyonlinelibrary.com]

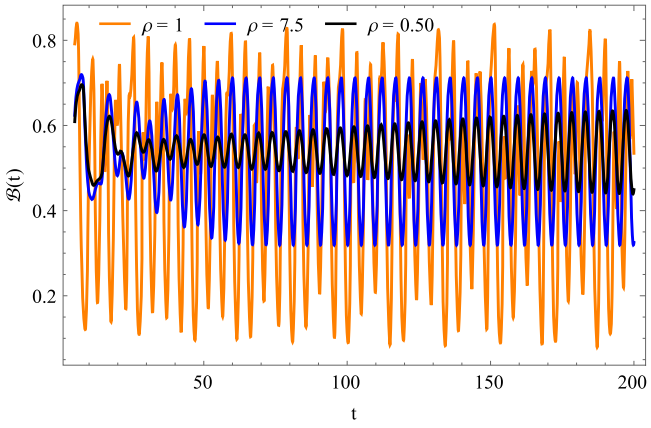

FIGURE 7 The power spectrum behavior of Equation (5) at $\alpha = 2$, $\mu = 0.8$, $\tau_1 = 1.8$, $\tau_2 = 6.2$, and $\kappa = 10$ for different ρ. [Colour figure can be viewed at wileyonlinelibrary.com]

Now, the above equation becomes with help of the Volterra integral equation

$$y(t) = \sum_{m=0}^{\nu-1} y_0^{(m)} \frac{t^m}{m!} + \frac{1}{\Gamma(\rho)} \int_0^t (t-s)^{\rho-1} \phi(s, y(s)) ds. \tag{23}$$

The ABM technique at $h = \frac{T}{N}$, $t_n = nh$, $n \in Z^+$ is derived in [50] to integrate Equation (23). System (4) becomes

$$D_t^\rho \mathcal{B}(t) = \frac{\alpha\, \mathcal{B}(t-\tau)}{1 + \mathcal{B}(t-\tau)^\kappa} - \mu \mathcal{B}(t). \tag{24}$$

Then

$$\begin{aligned} \mathcal{B}_{n+1} = \mathcal{B}_0 &+ \frac{h^\rho}{\Gamma(\rho+2)} \left(\frac{\alpha\, \mathcal{B}_{n+1}^H(t-\tau)}{1 + \mathcal{B}_{n+1}^H(t-\tau)^\kappa} - \mu \mathcal{B}_{n+1}^H(t) \right) \\ &+ \frac{h^\rho}{\Gamma(\rho+2)} \sum_{i=0}^{n} a_{i,n+1} \left(\frac{\alpha\, \mathcal{B}_i(t-\tau)}{1 + \mathcal{B}_i(t-\tau)^\kappa} - \mu \mathcal{B}(t) \right). \end{aligned} \tag{25}$$

Here

$$a_{i,n+1} = \begin{cases} n^{\rho+1} - (n-\rho)(n+1)^\rho, & i = 0, \\ (n-i+2)^{\rho+1} + (n-i)^{\rho+1} - 2(n-i+1)^{\rho+1}, & 1 \le i \le n, \\ 1, & i = n+1, \end{cases} \tag{26}$$

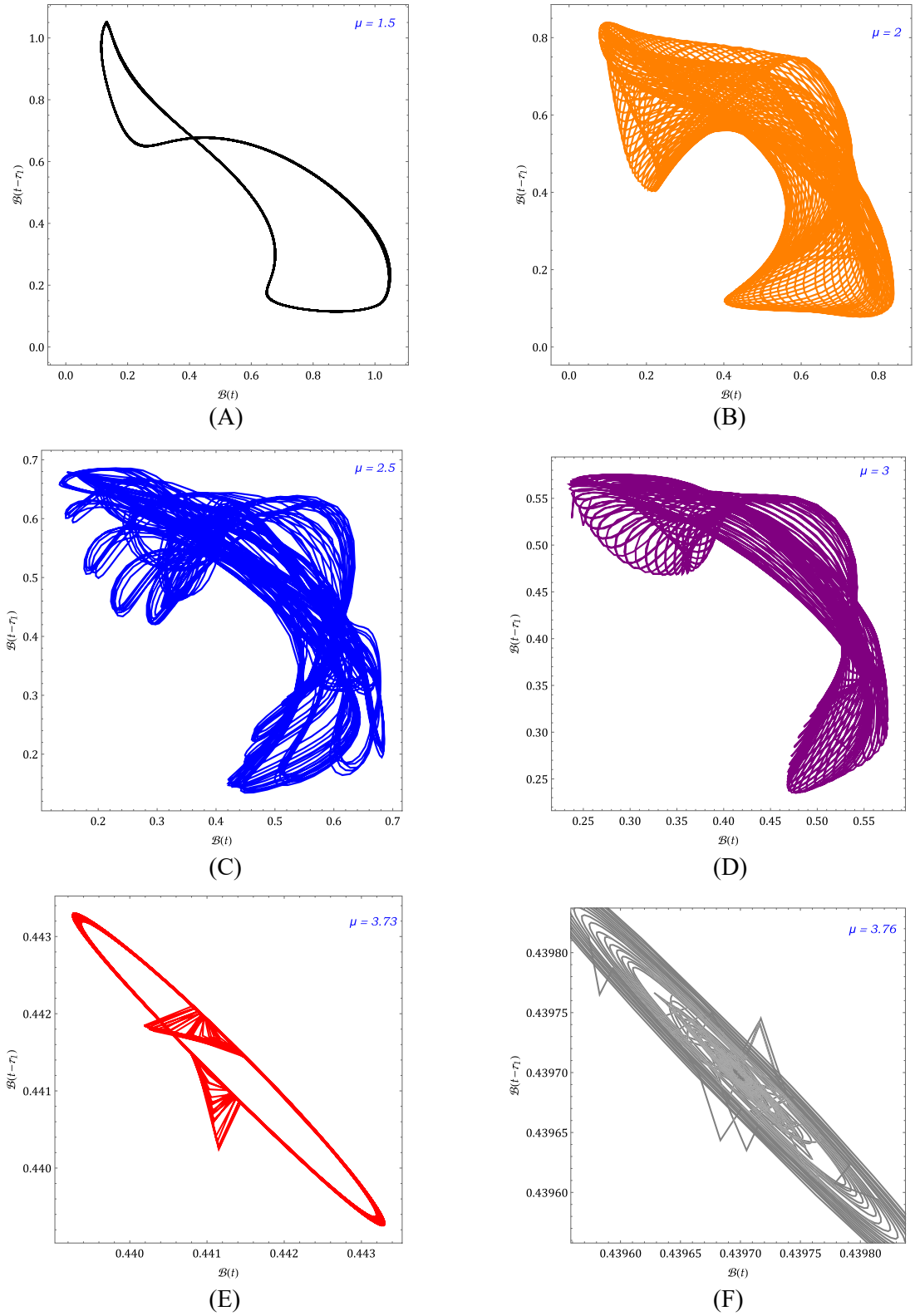

FIGURE 8 Parametric nature for Equation (5) at μ is (A) 1.5, (B) 2, (C) 2.5,(D) 3, (E) 3.73, and (F) 3.76 combined with $\kappa = 10, \tau_1 = 2.4, \tau_2 = 6.2, \rho = 1$, and $\alpha = 2$. [Colour figure can be viewed at wileyonlinelibrary.com]

and

$$b_{i,n+1} = \frac{h^\rho}{\rho}\left((n-i+1)^\rho - (n-i)^\rho\right), \ 0 \le i \le n. \tag{27}$$

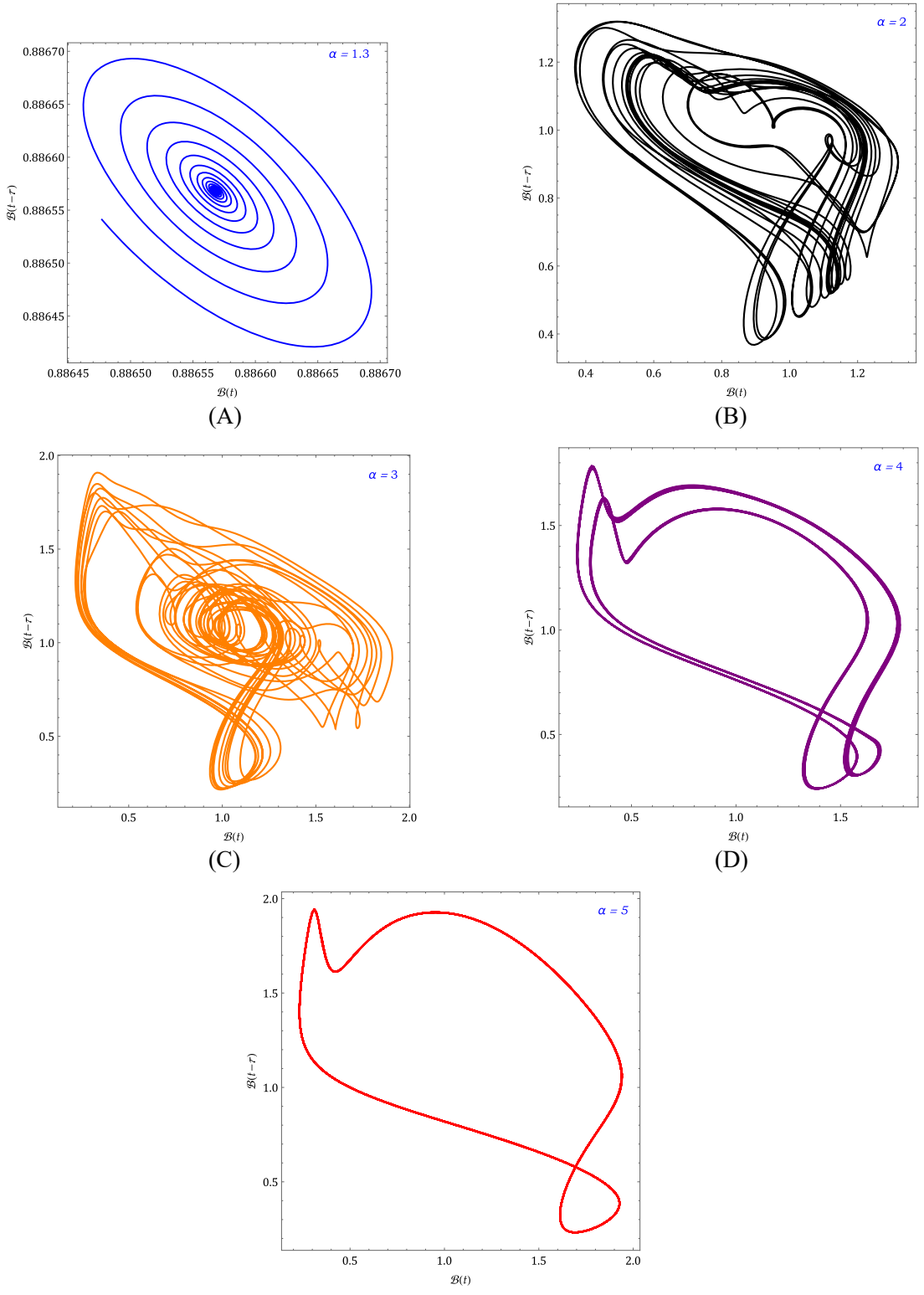

FIGURE 9 Parametric nature for Equation (4) at α is (A) 1.3, (B) 2, (C) 3, (D) 4, and (E) 5 combined with $\kappa = 10, \tau = 2, \mu = 1$, and $\rho = 1$. [Colour figure can be viewed at wileyonlinelibrary.com]

6 | RESULTS AND DISCUSSION

A bifurcation diagram illustrates the qualitative shifts in behavior that occur when a parameter is altered in a dynamical system. It is used to investigate if equilibrium and periodic orbits are stable and whether chaos exists in the system. Bifurcation diagrams are helpful because they illustrate how little changes in a system may have a big impact on how it behaves. In this connection, the bifurcation behavior for Equation (4) is cited in Figure 1. In a chaotic behavior plot, the state of a system is represented as a point in phase space. The system's phase space route is shown over time. The resultant plot is known as an analytic plot because it shows how the system is attracted to certain states in phase space. For Equation (4), chaotic nature is presented in Figure 2 and effect delay is drawn in Figure 3. The power spectrum can be used to investigate the periodic behavior of a solution in a differential equation context. The power spectrum in Figure 4 helps to investigate the periodic behavior of the blood cell population model for Equation (4). Equation (5) is captured the power spectrum in Figure 5. Time series graphs can reveal data anomalies, seasonality, patterns, and cycles. The time series Equation (4) in Figure 6 and for Equation (5) in Figure 7.

Since the systems having after-effect or dead time include hereditary systems, equations with diverging arguments, and functional differential equations. It has been captured in Figure 8 for Equation (5). The parameter α influences in extensive cases in the nature of the model which is the co-efficient of Equation (4), and its effect has been captured in Figure 9. These figures help us to understand the significance of fractional order and time delay in biological, mainly real-world problems to capture more inside behaviors. These behaviors are quite essential and not possible to capture using classical models. Further, this helps to understand the effect of delay changes can bring more complexity as delay increased for certain values.

7 | CONCLUSION

The mathematical model which describes the hematopoiesis (called the Mackey–Glass model) is examined with the help of the Caputo operator. The system is associated with more complex behavior due fact of its parameters and blood cells with delayed production rate. Two cases are considered to add more delay and which are captured in figures. In a chaotic behavior plot, the state of a system is represented as a point in phase space. The system's phase space route is shown over time. The resultant plot is known as a numerical plot because it shows how the system is attracted to certain states in phase space. We presented the theoretical acceptance including the condition for existence and then we captured the range for bifurcation. Also, we have drawn the power spectrum for both cases. The current investigation can help us to illustrate the system associated with parameters representing blood diseases. The present study can help researchers to apply the considered numerical algorithm and the theory of FC to examine day-to-day issues to study the more interesting consequences and so on [56].

AUTHOR CONTRIBUTIONS

Shuai Zhang: Conceptualization. **Yaya Wang:** Conceptualization. **Hongyin Geng:** Investigation. **Wei Gao:** Validation. **Esin Ilhan:** Writing—original draft. **Haci Mehmet Baskonus:** Methodology; data curation; investigation.

CONFLICT OF INTEREST STATEMENT

This work does not have any conflict of interest.

ORCID

Wei Gao https://orcid.org/0000-0001-7963-3502
Esin Ilhan https://orcid.org/0000-0002-0839-0942
Haci Mehmet Baskonus https://orcid.org/0000-0003-4085-3625

REFERENCES

1. G. Boubekeur, A. Ciancio, A. Moussa, L. Alhakim, and Y. Mati, *New analytical solutions and modulation instability analysis for the nonlinear (1+ 1)-dimensional Phi-four model*, Int. J. Math. Comput. Eng. **1** (2023), no. 1, 79–90.
2. E. Ata and I. O. Kıymaz, *New generalized Mellin transform and applications to partial and fractional differential equations*, Int. J. Math. Comput. Eng. **1** (2023), no. 1, 45–66.

3. J. Lu, L. Zhu, and W. Gao, *Remarks on bipolar cubic fuzzy graphs and its chemical applications*, Int. J. Math. Comput. Eng. **1** (2023), no. 1, 1–9.
4. D. V. Bhise, S. A. Choudhari, M. A. Kumbhalkar, and M. M. Sardeshmukh, *Modelling the critical success factors for advanced manufacturing technology implementation in small and medium sized enterprises*, 3c Empresa: Investigacion y Pensamiento Crí,tico **11** (2022), no. 2, 263–275.
5. W. Gao, P. Veeresha, C. Cattani, C. Baishya, and H. M. Baskonus, *Modified predictor-corrector method for the numerical solution of a fractional-order SIR model with 2019-nCoV*, Fractal Fract. **6** (2022), no. 2, 92.
6. M. P. Anilkumar and K. P. Jose, *Analysis of a discrete time queueing-inventory model with back-order of items*, 3c Empresa: Investigació,n y Pensamiento Crítico **11** (2022), no. 2, 50–62.
7. E. N. Lorenz, *Deterministic nonperiodic flow*, J. Atmos. Sci. **20** (1963), no. 2, 130–141.
8. P. Veeresha, *The efficient fractional order based approach to analyze chemical reaction associated with pattern formation*, Chaos Solitons Fract. **165** (2023), 112862.
9. M. Naik and C. Baishya, *Design of a fractional-order atmospheric model via a class of ACT-like chaotic system and its sliding mode chaos control*, Chaos **33** (2023), 023129.
10. H. Mohammadi, S. Kumar, S. Rezapour, and S. Etemad, *A theoretical study of the Caputo-Fabrizio fractional modeling for hearing loss due to Mumps virus with optimal control*, Chaos, Solitons Fract. **144** (2021), 110668.
11. A. Chakraborty and P. Veeresha, *Investigating the dynamics, synchronization and control of chaos within a transformed fractional Samardzija-Greller framework*, Chaos, Solitons Fract. **182** (2024), 114810.
12. D. Baleanu, S. M. Aydogn, H. Mohammadi, and S. Rezapour, *On modelling of epidemic childhood diseases with the Caputo-Fabrizio derivative by using the Laplace Adomian decomposition method*, Alex. Eng. J. **59** (2020), no. 5, 3029–3039.
13. H. Khan, K. Alam, H. Gulzar, S. Etemad, and S. Rezapour, *A case study of fractal-fractional tuberculosis model in China: Existence and stability theories along with numerical simulations*, Math. Comput. Simul. **198** (2022), 455–473.
14. D. Baleanu, S. Etemad, H. Mohammadi, and S. Rezapour, *A novel modeling of boundary value problems on the glucose graph*, Commun. Nonlinear Sci. Numer. Simul. **100** (2021), 105844.
15. D. Baleanu, A. Jajarmi, H. Mohammadi, and S. Rezapour, *A new study on the mathematical modelling of human liver with Caputo-Fabrizio fractional derivative*, Chaos, Solitons Fract. **134** (2020), 109705.
16. N. H. Tuan, H. Mohammadi, and S. Rezapour, *A mathematical model for COVID-19 transmission by using the Caputo fractional derivative*, Chaos, Solitons Fract. **140** (2020), 110107.
17. A. Chakraborty and P. Veeresha, *Effects of global warming, time delay and chaos control on the dynamics of a chaotic atmospheric propagation model within the frame of Caputo fractional operator*, Commun. Nonlinear Sci. Numer. Simul. **128** (2024), 107657.
18. S. Hussain, E. N. Madi, H. Khan, H. Gulzar, S. Etemad, S. Rezapour, and M. K. Kaabar, *On the stochastic modeling of COVID-19 under the environmental white noise*, J. Funct. Spaces **1** (2022), 4320865.
19. M. Ahmad, A. Zada, M. Ghaderi, R. George, and S. Rezapour, *On the existence and stability of a neutral stochastic fractional differential system*, Fractal Fract. **6** (2022), no. 4, 203.
20. V. Raghavendra and P. Veeresha, *Analysing the market for digital payments in India using the predator-prey mode*, An Int. J. Optim. Control: Theor. Appl. (IJOCTA) **13** (2023), no. 1, 104–115.
21. H. Khan, J. Alzabut, A. Shah, Z. Y. He, S. Etemad, S. Rezapour, and A. Zada, *On fractal-fractional waterborne disease model: A study on theoretical and numerical aspects of solutions via simulations*, Fractals **31** (2023), no. 04, 2340055.
22. S. M. Aydogan, D. Baleanu, H. Mohammadi, and S. Rezapour, *On the mathematical model of Rabies by using the fractional Caputo-Fabrizio derivative*, Adv. Differ. Equa. **2020** (2020), no. 1, 382.
23. W. Gao, P. Veeresha, D. G. Prakasha, B. Senel, and H. M. Baskonus, *Iterative method applied to the fractional nonlinear systems arising in thermoelasticity with Mittag-Leffler kernel*, Fractals **28** (2020), no. 08, 2040040.
24. K. Dehingia, A. A. Mohsen, S. A. Alharbi, R. D. Alsemiry, and S. Rezapour, *Dynamical behavior of a fractional order model for within-host SARS-CoV-2*, Mathematics **10** (2022), no. 13, 2344.
25. S. Hussain, E. N. Madi, H. Khan, S. Etemad, S. Rezapour, T. Sitthiwirattham, and N. Patanarapeelert, *Investigation of the stochastic modeling of COVID-19 with environmental noise from the analytical and numerical point of view*, Mathematics **9** (2021), no. 23, 3122.
26. H. Khan, J. Alzabut, A. Shah, Z. Y. He, S. Etemad, S. Rezapour, and A. Zada, *On fractal-fractional waterborne disease model: a study on theoretical and numerical aspects of solutions via simulations*, Fractals **31** (2023), no. 04, 2340055.
27. M. C. Macke and L. Glass, *Oscillation and chaos in physiological control systems*, Science **197** (1977), 287–289.
28. S. Lynch and J. Borresen, Oscillations, feedback and bifurcations in mathematical models of angiogenesis and haematopoiesis, *Handbook of vascular biology techniques*, Slevin M, McDowell G, Cao Y, and Kitajewski J, (eds.), Springer, New York, 2015, pp. 373–390.
29. P. E. Rap, *An atlas of cellular oscillators*, J. Exp. Biol. **81** (1979), 281–306.
30. B. J. Altman, *Cancer clocks out for lunch: disruption of circadian rhythm and metabolic oscillation in cancer*, Front. Cell Dev. Bill. **4** (2016), 62, DOI 10.3389/fcell.2016.00062.
31. K. Chakraborty, M. Chakraborty, and T. K. Kar, *Bifurcation and control of a bioeconomic model of a prey-predator system with a time delay*, Nonlinear Anal.-Hybrid Syst. **5** (2011), 613–625.
32. H. Zhang, L. Chen, J. J. Nieto, and A delayed epidemic model with stagestructure and pulses for pest management strategy, Nonlin. Anal. Real World Appl. **9** (2008), 1714–1726.
33. S. Lynch, *Dynamical systems with applications using Mathematica*, Boston, Birkhäuser, 2007, pp. 363–385.

34. J. Liouville, *Memoire surquelques questions de geometrieet de mecanique, et sur un nouveau genre de calcul pour resoudreces questions*, J. Ecole. Polytech. **13** (1832), 1–69.
35. G. F. B. Riemann, *Versuch Einer Allgemeinen Auffassung der Integration und Differentiation*, Gesammelte Mathematische Werke, Leipzig, 1896.
36. M. Caputo, *Linear models of dissipation whose Q is almost frequency independent-II*, Geophys. J. Int. **13** (1967), no. 5, 529–539.
37. M. Caputo, *Elasticita e Dissipazione*, Zanichelli, Bologna, 1969.
38. K. S. Miller and B. Ross, *An introduction to fractional calculus and fractional differential equations*, A Wiley, New York, 1993.
39. I. Podlubny, *Fractional differential equations*, Academic Press, New York, 1999.
40. M. Caputo and M. Fabrizio, *A new definition of fractional derivative without singular kernel*, Prog. Fract. Differ. Appl. **1** (2015), no. 2, 73–85.
41. A. Atangana and D. Baleanu, *New fractional derivatives with non-local and non-singular kernel theory and application to heat transfer model*, Therm. Sci. **20** (2016), 763–769.
42. A. A. Kilbas, H. M. Srivastava, and J. J. Trujillo, *Theory and applications of fractional differential equations*, Elsevier, Amsterdam, 2006.
43. D. Baleanu, Z. B. Guvenc, and J. A. Tenreiro Machado, *New trends in nanotechnology and fractional calculus applications*, Springer Dordrecht Heidelberg London New York, 2010.
44. P. Veeresha and D. Baleanu, *A unifying computational framework for fractional Gross-Pitaevskii equations*, Phys. Scr. **96** (2021), no. 12, 125010.
45. L. Beghin and M. Caputo, *Commutative and associative properties of the Caputo fractional derivative and its generalizing convolution operator*, Commun. Nonlinear Sci. Numer. Simul. **89** (2020), 105338.
46. C. Baishya and P. Veeresha, *Laguerre polynomial-based operational matrix of integration for solving fractional differential equations with non-singular kernel*, Proc. Roy. Soc. A **477** (2021), 2253.
47. C. Li and C. Tao, *On the fractional Adams method*, Comput. Math. Appl. **58** (2009), no. 8, 1573–1588.
48. K. Diethelm, *An algorithm for the numerical solution of differential equations of fractional order*, Electron. Trans. Numer. Anal. **5** (1997), no. 1, 1–6.
49. K. Diethelm and N. J. Ford, *Analysis of fractional differential equations*, J. Math. Anal. Appl. **265** (2002), no. 2, 229–248.
50. K. Diethelm, N. J. Ford, and A. D. Freed, *A predictor-corrector approach for the numerical solution of fractional differential equations*, Nonlinear Dyn. **29** (2002), no. 1, 3–22.
51. B. S. T. Alkahtani, A. Atangana, and I. Koca, *Novel analysis of the fractional Zika model using the Adams type predictor-corrector rule for non-singular and non-local fractional operators*, J. Nonlinear Sci. Appl. **10** (2017), no. 6, 3191–3200.
52. I. Podlubny, *Fractional differential equations*, Academic Press, San Diego, 1999.
53. B. Wang and L.-Q. Chen, *Asymptotic stability analysis with numerical confirmation of an axially accelerating beam constituted by the standard linear solid model*, J. Sound Vib. **328** (2009), no. 4-5, 456–466.
54. H.-L. Li, L. Zhang, C. Hu, Y.-L. Jiang, and Z. Teng, *Dynamical analysis of a fractional-order predator-prey model incorporating a prey refuge*, J. Appl. Math. Comput. **54** (2017), no. 1, 435–449.
55. M. Martcheva, *An introduction to mathematical epidemiology*, Springer, New York, 2015, pp. 61.
56. O. Ilhan and G. Sahin, *A numerical approach for an epidemic SIR model via Morgan-Voyce series*, Int. J. Math. Comput. Eng. **2** (2024), no. 1, 125–140.

How to cite this article: S. Zhang, Y. Wang, H. Geng, W. Gao, E. Ilhan, and H. M. Baskonus, *On the analyzing of bifurcation properties of the one-dimensional Mackey–Glass model by using a generalized approach*, Math. Meth. Appl. Sci. (2024), 1–15, DOI 10.1002/mma.10381.